§1. Estimation of Partial Carbon Radiation at each Ionization Stage of C^{2+} to C^{5+} Ions in LHD

Morita, S., Oishi, T., Murakami, I., Huang, X.L., Goto, M., Zhang, H.M., Liu, Y. (SOKENDAI)

Study of the impurity radiation is important to clarify the physical mechanism triggering the RMP-assisted detachment in LHD. For the purpose resonance lines of CIII (977.02 Å, 2s2p – $2s^2$), CIV (1548.2 Å, 2p – 2s), CV (40.27 Å, 1s2p – $1s^2$) and CVI (33.73 Å, 2p – 1s) measured by VUV and EUV spectrometers are used to estimate the radiation power from C^{2+} – C^{5+} ions. The spectral intensity from the VUV spectrometer is absolutely calibrated using the EUV spectrometer with which the intensity has been already calibrated. The partial carbon radiation at each ionization stage of C^{2+} to C^{5+} ions, P_{rad} (C^{q+}), can be then estimated for attached and detached plasmas by calculating a ratio of the partial carbon radiation to the resonance line based on ADAS atomic code. It is found that the radiation from C^{3+} ions existing near a radial location of $\iota/2\pi = 1$ in the ergodic layer increases up to 40% of the total radiation loss, while the carbon radiation is negligibly small in the attached plasma.[1)]

Radiation power of the resonance transition generally occupies a considerably large part in the radiation power from impurity ions in a certain ionization stage. Since the absolute intensity of resonance line of CIII (977.02 Å), CIV (1548.2 Å), CV (40.27 Å) and CVI (33.73 Å) is measured with the EUV and VUV spectrometers, the ratio of P_{rad} (C^{q+}) to resonance line intensity in C^{q+} ions can be calculated with ADAS atomic code. The ratio of P_{rad} (C^{q+}) to resonance line intensity is shown in Figs. 1(a)–(d) as a function of electron temperature with parameter of electron density. Since the ratio is practically insensitive to n_e as seen in the figure, the contribution of n_e can be neglected in the present analysis. As the value of T_e for each ionization stage of carbon ions is already determined, the P_{rad} (C^{q+}) can be evaluated from the intensity ratio.

The P_{rad} (C^{2+}) to P_{rad} (C^{5+}) are analyzed for attached and detached plasmas. Figure 2 shows a comparison of discharge waveform between attached and detached plasmas. The total radiation loss, P_{rad}, shows similar values for both plasmas, i.e. 20–25% to the port-through NBI power, P_{NBI}. In the attached plasma the contribution of P_{rad} (C^{2+}) and P_{rad} (C^{4+}) to P_{rad} is less than 1%, while P_{rad} (C^{3+})/P_{rad} and P_{rad} (C^{5+})/P_{rad} are 8% and 2%, respectively. In the detached plasma, it is found that the P_{rad} (C^{2+})/P_{rad} and P_{rad} (C^{3+})/P_{rad} significantly increase to 3% and 40% during the detachment phase, respectively, whereas the increment of P_{rad} is only 300 kW. In contrast, the P_{rad} (C^{4+})/P_{rad} and P_{rad} (C^{5+})/P_{rad} do not change so much compared to the attached plasma.

The drastic increase in P_{rad} (C^{2+}) and P_{rad} (C^{3+}) during the detachment phase is very clear from the present analysis. The P_{rad} (C^{3+}) expresses a dominant portion in the total carbon radiation in the detached plasma. A flattening of T_e profile appears during the detachment phase in edge T_e of 10 ~ 20 eV at the radial location of m/n = 1/1 magnetic island. Radial locations of C^{2+} and C^{3+} ions are also broadened reflecting the T_e flattening. The expansion of the radial location significantly enhances the P_{rad} (C^{2+}) and P_{rad} (C^{3+}) in the detached plasma. Therefore, it is concluded that a change in the edge transport of C^{2+} and C^{3+} ions locating near m/n = 1/1 island brought by the RMP field play an important role for the present detachment achievement. In addition, the carbon transport near LCFS is not affected by the supplied RMP field because the P_{rad} (C^{4+}) and P_{rad} (C^{5+}) do not change at all in both discharges with attachment and detachment.

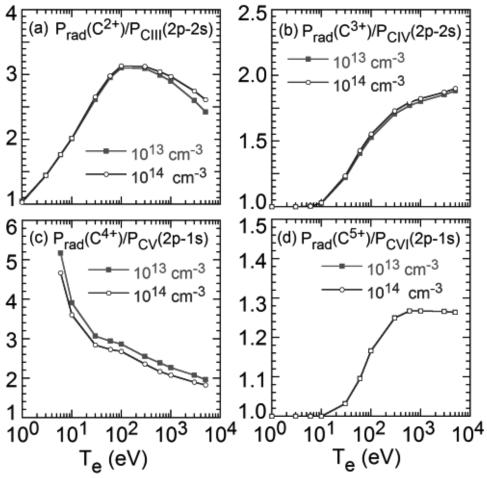

Fig. 1. Ratios of partial carbon radiation power at each ionization stage to radiation power of resonance line calculated with ADAS atomic code: (a) P_{rad} (C^{2+})/P_{CIII} (2p-2s), (b) P_{rad} (C^{3+})/P_{CIV} (2p-2s), (c) P_{rad} (C^{4+})/P_{CV} (2p-1s) and (d) P_{rad} (C^{5+})/P_{CVI} (2p-1s).

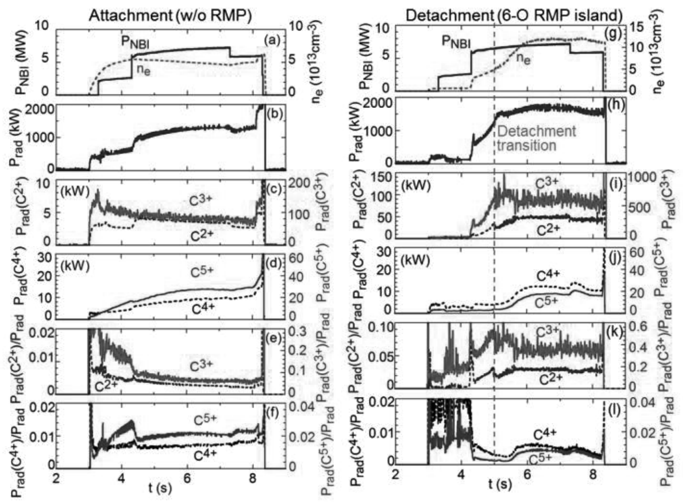

Fig. 2. Time behaviors of (a) NBI port-through power and line-averaged electron density, (b) total radiation loss (P_{rad}), partial carbon radiation power of (c) P_{rad} (C^{2+}) and P_{rad} (C^{3+}) and (d) P_{rad} (C^{4+}) and P_{rad} (C^{5+}) and ratios of P_{rad} (C^{q+}) to P_{rad} of (e) P_{rad} (C^{2+})/P_{rad} and P_{rad} (C^{3+})/P_{rad} and (f) P_{rad} (C^{4+})/P_{rad} and P_{rad} (C^{5+})/P_{rad} in the attached plasma without RMP. Graphs of (g) - (l) indicate time behaviors from detached plasma with 6-O RMP island in the same meaning as graphs (a) - (f).

1) Zhang, H.M. et al., Plasma. Fus. Res. **11** (2016) 2402019.